Supporting Information

Photochemical Synthesis of Group 10 Metal Nanoclusters for Electrocatalysis

Ji-Qiang Fan,[a] Kehui Cen,[b] Hua-Jun Xu,[c] Hai-Yang Wang,[c] Ying Yang,[d] Ze-Min Zhu,[a] Hao Liu,[a] Dengyu Chen,[b] Weigang Fan,*[a] Man-Bo Li*[a]

[a] Institutes of Physical Science and Information Technology, Key Laboratory of Structure and Functional Regulation of Hybrid Materials of Ministry of Education, Anhui University, Hefei 230601 (P. R. China).

[b] Co-Innovation Center of Efficient Processing and Utilization of Forest Resources, College of Materials Science and Engineering, Nanjing Forestry University, Nanjing 210037, China

[c] Technology Center, China Tobacco Anhui Industrial Co., Ltd., 9 Tianda Road, Hefei 230088 (P. R. China)

[d] College of Materials and Chemical Engineering, West Anhui University, Lu'an, Anhui 237015 (P. R. China)

* Corresponding Authors: weigang.fan@ahu.edu.cn; mbli@ahu.edu.cn

Table of Contents

Materials and characterizations

Dichloromethane (DCM 99.0%), toluene (Tol, 99.0%), methanol (MeOH, 99.5%), ethanol (EtOH, 99.5%), ethyl acetate (EA, 99.0%), n-hexane (99.0%), petroleum ether (PE, 99.0%) and tetrahydrofuran (THF, 99.0%) were purchased from Sinopharm Chemical Reagent Co. Ltd. Sodium borohydride ($NaBH_4$) was purchased from Shanghai Chemical Reagent Co. Ltd. Diphenyl disulfide (PhSSPh) and p-Tolyl disulfide were purchased from Aladdin Co. Ltd. Nickel(II) acetylacetonate, bis(triphenylphosphine)nickel(II)chloride and palladium acetate ($Pd(OAc)_2$) were purchased from Adamas. All the water used in experiments is ultrapure produced by AIC pure water system. All chemicals were used without further purification. All glassware was thoroughly cleaned with aqua regia (HCl/HNO_3 3/1 v/v), rinsed with copious amounts of pure water, and then dried in an oven prior to use.

The single crystal X-ray diffraction (SCXRD) was carried out on an STOE STADIVARI diffractometer under liquid nitrogen flow at 173 K, using a Mo Kα (λ = 0.71073) for $Pd_{10}(SPh)_{20}$ and $Pd_9(SPh)_{18}$, and a Cu Kα (λ = 1.54186 Å) for $Ni_{11}(SPh)_{22}$ and $Ni_{10}(4\text{-}MePhS)_{20}$, respectively. Data reductions and absorption corrections were performed using SAINT (Bruker) and SHELXTL (Bruker, 2008), respectively. The structures were solved by direct methods and refined with full-matrix least-squares on F^2 using the SHELXL-2014/7 (Sheldrick, 2014) suite of programs. The placement of the heteroatoms was ascertained by the method of modifying the disorderly free variables. All UV-vis absorption measurements were performed on a SPECORD 210 PLUS spectrophotometer at room temperature. Electrospray ionization mass spectrum (ESI-MS) was acquired on a Waters Q-TOF mass spectrometer equipped with a Z-spray source. The sample was directly infused into the chamber at 5 μL/min. CV of metal nanoclusters were performed with an electrochemical workstation (CHI 700E). A glassy carbon electrode was used as the working electrode, which was polished with 0.015 μm Al_2O_3 slurries, ultrasonically rinsed with EtOH for 5 minutes, washed with nanopure water, and carefully dried with a cold air stream. A Pt wire and an Ag/AgCl electrode were used as the counter

electrode and the reference electrode, respectively. The metal nanocluster (3-5 mg) was dissolved in 5 mL DCM containing n-Bu_4NPF_6 (0.1 M). After the test, the glassy carbon electrode was re-polished and the rest of the electrodes were washed and dried for the next experiment.

Photochemical synthesis of group 10 metal nanoclusters

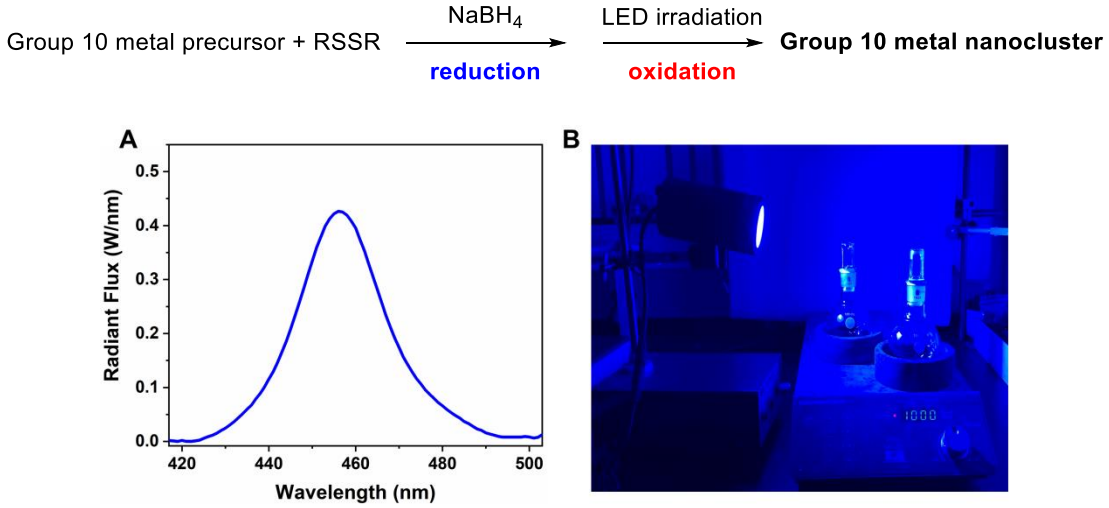

Figure S1. (A) The electroluminescent spectrum of the LED used. (B) The irradiation setup.

(1) Synthesis of $Ni_{11}(SPh)_{22}$

Nickel(II) acetylacetonate and PhSSPh were used as the metal precursor and disulfide, respectively, for the synthesis of $Ni_{11}(SPh)_{22}$.

Nickel(II) acetylacetonate (77.0 mg, 0.30 mmol) dissolved in 3 mL methanol was added into a 100 mL round-bottom flask with 15 mL THF under stirring at 1000 rpm. PhSSPh (131 mg, 0.60 mmol) was then added and the mixture was stirred for 20 min. $NaBH_4$ (56.7 mg, 1.50 mmol) dissolved in 3 mL of ice-cold water was immediately added into the system. The resulted mixture was stirred at room temperature under a 25 W blue LED for 8 h. After completion of the reaction, the solvent was removed under reduced pressure. The as-obtained residue was washed three times by MeOH to ensure any excess reactants being removed. The crude products were purified by recrystallization to obtain the pure $Ni_{11}(SPh)_{22}$ (18.3 mg, 22% yield, based on Ni atom). Black rhombic crystals suitable for SCXRD were achieved by slow evaporation of the purified product in DCM/EtOH solution.

(2) Control experiments

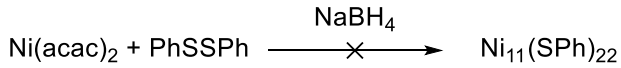

Nickel(II) acetylacetonate (77.0 mg, 0.30 mmol) dissolved in 3 mL methanol was added into a 100 mL round-bottom flask with 15 mL THF under stirring at 1000 rpm. PhSSPh (131 mg, 0.60 mmol) was then added and the mixture was stirred for 20 min. $NaBH_4$ (56.7 mg, 1.50 mmol) dissolved in 3 mL of ice-cold water was immediately added into the system. The resulting solution was stirred for 8 h. Black Ni particles were obtained instead of $Ni_{11}(SPh)_{22}$, which were not dissolvable in normal solvents, such as DCM, MeOH, EtOH, and toluene.

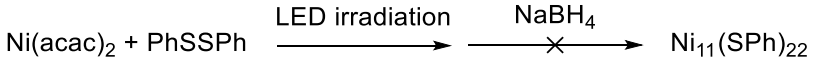

Nickel(II) acetylacetonate (77.0 mg, 0.30 mmol) dissolved in 3 mL methanol was added into a 100 mL round-bottom flask with 15 mL THF under stirring at 1000 rpm. PhSSPh (131 mg, 0.60 mmol) was added and the mixture was stirred under a 25 W blue LED. Afterwards, $NaBH_4$ (56.7 mg, 1.50 mmol) dissolved in 3 mL of ice-cold water was immediately added into the system. The resulting solution was stirred for 8 h. Black Ni particles were obtained instead of $Ni_{11}(SPh)_{22}$, which were not dissolvable in normal solvents, such as DCM, MeOH, EtOH, and toluene.

(3) Large-scale synthesis

Nickel(II) acetylacetonate (4.18 g, 16.3 mmol) dissolved in 80 mL methanol was added into 500 mL THF under stirring at 1500 rpm. PhSSPh (7.12 g, 32.6 mmol) was then added and the mixture was stirred for 40 min. $NaBH_4$ (3.08 g, 81.5 mmol) dissolved in 80 mL of ice-cold water was immediately added into the system. The resulted mixture was stirred at room temperature under a 25 W blue LED for 24 h. After completion of the reaction, insoluble precipitates were removed by centrifugation. The solvent was removed under reduced pressure. The as-obtained residue was washed three times by MeOH to ensure any excess reactants being removed. The crude products were further purified by recrystallization to obtain pure $Ni_{11}(SPh)_{22}$ (1.005 g, 22% yield, based on Ni atom).

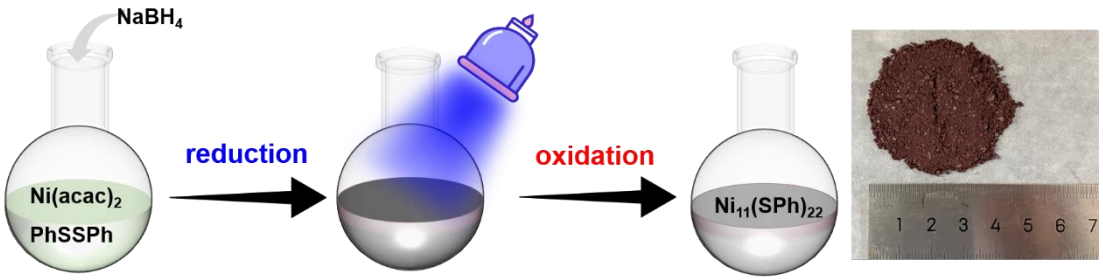

Figure S2. Illustration of the large-scale synthesis, and the photograph of the as-obtained Ni_{11} nanocluster.

(4) Synthesis of $Ni_{10}(4\text{-MePhS})_{20}$

Nickel(II) acetylacetonate and 4-methylphenyl disulfide were used as the metal precursor and disulfide, respectively, for the synthesis of $Ni_{10}(4\text{-MePhS})_{20}$.

Nickel(II) acetylacetonate (77.0 mg, 0.30 mmol) dissolved in 3 mL methanol was added into a 100 mL round-bottom flask with 15 mL THF under stirring at 1000 rpm. 4-methylphenyl disulfide (148 mg, 0.60 mmol) was then added and the mixture was stirred for 20 min. $NaBH_4$ (56.7 mg, 1.50 mmol) dissolved in 3 mL of ice-cold water was immediately added into the system. The resulted mixture was stirred at room temperature under a 25 W blue LED for 8 h. After the completion of the reaction, the solvent was removed under reduced pressure. The as-obtained residue was washed three times by MeOH to ensure any excess reactants being removed. The crude products were purified by recrystallization to obtain the pure $Ni_{10}(4\text{-MePhS})_{20}$ (23.8 mg, 26% yield, based on Ni atom). Black rhombic crystals suitable for SCXRD were achieved by slow evaporation of the purified product in DCM/EtOH solution.

(5) Synthesis of $Pd_9(SPh)_{18}$

Palladium acetate and PhSSPh were used as the metal precursor and disulfide, respectively, for the synthesis of $Pd_9(SPh)_{18}$.

$Pd(OAc)_2$ (33.0 mg, 0.15 mmol) dissolved in 3 mL methanol was added into a 100 mL round-bottom flask with 15 mL THF under stirring at 1000 rpm. PhSSPh (131 mg, 0.60 mmol) was then added and the mixture was stirred for 20 min. $NaBH_4$ (28.3 mg, 0.75 mmol) dissolved in 3 mL of ice-cold water was immediately added into the

system. The resulted mixture was stirred at room temperature under a 25 W blue LED for 8 h. After the completion of the reaction, the solvent was removed under reduced pressure. The as-obtained residue was washed three times by MeOH to ensure any excess reactants being removed. The crude products were purified by recrystallization to obtain the pure $Pd_9(SPh)_{18}$ (7.31 mg, 15% yield, based on Pd atom). Red rhombic crystals suitable for SCXRD were achieved by slow evaporation of the purified product in DCM/EtOH solution.

(6) Synthesis of $Pd_{10}(SPh)_{20}$

Palladium acetate and PhSSPh were used as the metal precursor and disulfide, respectively, for the synthesis of $Pd_{10}(SPh)_{20}$.

$Pd(OAc)_2$ (33.0 mg, 0.15 mmol) was dissolved into 20 mL methanol in a 100 mL round-bottom flask. PhSSPh (65.5 mg, 0.30 mmol) was then added and the mixture was stirred for 15 min. $NaBH_4$ (28.3 mg, 0.75 mmol) dissolved in 3 mL of ice-cold water was immediately added into the system. The resulted mixture was stirred at room temperature under a 25 W blue LED for 5 h. After the completion of the reaction, the solvent was removed under reduced pressure. The as-obtained residue was washed three times by MeOH to ensure any excess reactants being removed. The crude products were purified by recrystallization to obtain the pure $Pd_{10}(SPh)_{20}$ (5.36 mg, 11% yield, based on Pd atom). Red rhombic crystals suitable for SCXRD were achieved by slow evaporation of the purified product in DCM/EtOH solution.

Group 10 metal nanoclusters catalyzed ORR

(1) Synthesis of $Ni(SR)_2$ and $Ni_6(SR)_{12}$

Nickel chloride hexahydrate (100 mg, 0.42 mmol) dissolved in 3mL methanol was added into a 100 mL round-bottom flask with 15 mL THF under stirring at 1000 rpm. 2-Phenylethanethiol (280 uL, 2.03 mmol) was then added and the mixture was stirred for 15 min. Subsequently 50 μL of triethylamine was added to the system. The resulted mixture was stirred for 2 h. After the completion of the reaction, the solvent was removed under reduced pressure. The as-obtained residue was washed three times by MeOH to ensure any excess reactants being removed. The obtained $Ni(SR)_2$ complex was used directly.

Nickel chloride hexahydrate (100 mg, 0.42 mmol) dissolved in 3mL methanol was added into a 100 mL round-bottom flask with 15 mL THF under stirring at 1000 rpm. 2-Phenylethanethiol (280 uL, 2.03 mmol) was then added and the mixture was stirred for 10 min. $NaBH_4$ (38.0 mg, 1.00 mmol) dissolved in 3 mL of ice-cold water was immediately added into the system. The resulted mixture was stirred for 3 h. After the completion of the reaction, the solvent was removed under reduced pressure. The as-obtained residue was washed three times by MeOH to ensure any excess reactants being removed. The crude products were purified by recrystallization to obtain the pure $Ni_6(SR)_{12}$.[1]

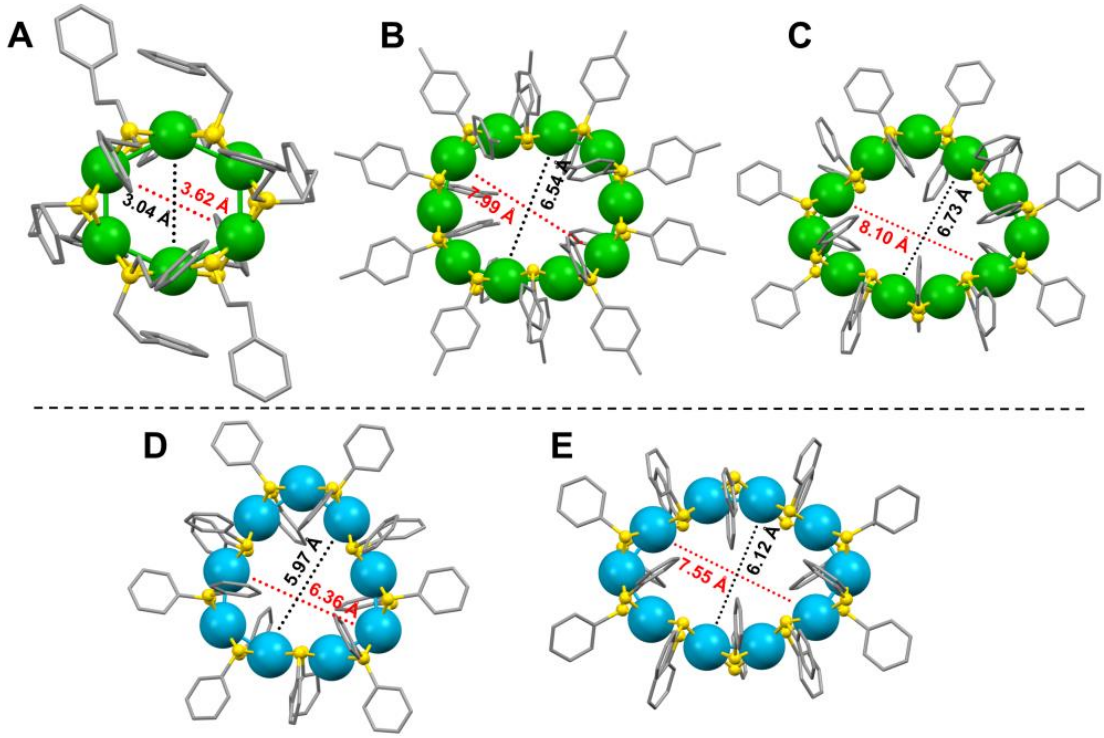

Figure S3. The structure and cavity size of Ni_6, Ni_{10}, Ni_{11}, Pd_9 and Pd_{10}.

(2) Preparation of carbon-supported $Ni(SR)_2$, $Ni_6(SR)_{12}$, $Ni_{10}(4\text{-}MePhS)_{20}$, $Ni_{11}(SPh)_{22}$, $Pd_9(SPh)_{18}$ and $Pd_{10}(SPh)_{20}$

45 mg of carbon black was dispersed in 20 mL of DCM and then stirred at 1000 rpm in a 100 mL round bottom flask. 5 mg of each nanocluster mentioned above was dried under N_2 and added into the carbon black solution to form a 10 wt% carbon-supported nanocluster catalyst in 24 h at 1000 rpm. The as-prepared catalyst was dried under a gentle N_2 stream and stored at room temperature for the further use.

(3) Catalytic experiments

10 mg of carbon-supported metal nanocluster was evenly dispersed in a suspension including 300 μL of isopropanol, 700 μL of deionized water and 50 μL of 5 wt% Nafion solutions by ultrasonication. Afterward, 8 μL of the ink was placed on a glassy carbon rotating disk electrode (5 mm in diameter, 0.196 cm^2) by using a micro syringe and was thoroughly dried at room temperature.

ORR were carried out on a CHI 660E electrochemical workstation using a three-electrode system, in which a Pt wire was used as the counter electrode, an

Ag/AgCl electrode was employed as the reference electrode (in the saturated state of KCl) and a rotating disk electrode (RDE) containing catalyst ink on the glassy carbon (GC) was used as the working electrode. The electrolyte was an oxygen-saturated 0.1 M KOH solution prepared with nanopure water. Oxygen saturation was achieved by bubbling with O_2 gas for more than 30 min. The measured potentials are referred to the RHE, $E_{RHE} = E_{Ag/AgCl} + 0.059\ pH + E^{\theta}_{Ag/AgCl}$. The catalyst inks were produced as the following: 10 mg of carbon-supported metal nanocluster catalysts powder were evenly dispersed in a suspension including 300 μL of isopropanol, 700 μL of deionized water and 50 μL of 5 wt% Nafion solutions by ultrasonication. Afterward, 8 μL of the ink was placed on a glassy carbon rotating disk electrode (5 mm in diameter, 0.196 cm^2) by using a micro syringe and was thoroughly dried at room temperature.

CV measurements for ORR were performed from -0.77 to 0.03 V at a scan rate of 10 mV s^{-1} in O_2-saturated electrolyte. In order to measure the electrochemical performances of the carbon-supported nanocluster catalysts for ORR, the LSV carves were observed from -0.8 V to 0.2 V (vs. Ag/AgCl) at a scan rate of 10 mV s^{-1} at different rotation rates (400-2500 rpm) in O_2-saturated electrolyte. The electron transfer number (n) per O_2 molecule for ORR can be determined by the slopes of the Koutecky-Levich (K-L) plot, as shown in the following formulas:

$$\frac{1}{j} = \frac{1}{j_K} + \frac{1}{j_L} = \frac{1}{j_K} + \frac{1}{B \times \omega^{1/2}}$$

$$B = 0.2 \times n \times F \times C_{O_2} \times D_{O_2}^{\frac{2}{3}} \times V^{-\frac{1}{6}}$$

In the above, j is the measured current density, j_K is the dynamic current density, j_L is the diffusion limiting, ω is the electrode speed, n is the number of electron transfer in the ORR, F is the Faraday constant (96485 C mol^{-1}), C_{O2} is the saturated oxygen concentration in the 0.1 M KOH aqueous solution (1.2×10^{-6} mol cm^{-3}), D_{O2} is the oxygen diffusion coefficient (1.9×10^{-5} cm^2 s^{-1}), and v is the kinematic viscosity of the solution (0.01 cm^2 s^{-1}).

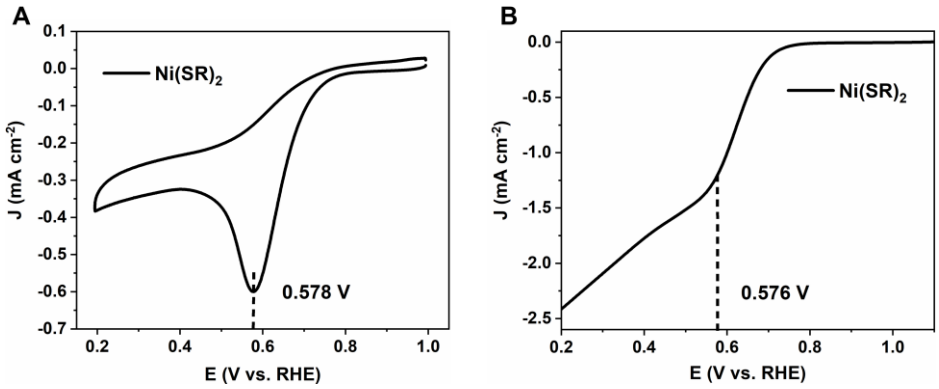

Figure S4. (A) CV curves of $Ni(SR)_2$ in O_2-saturated 0.1 M KOH. (B) LSV polarization curves of $Ni(SR)_2$ in 0.1 M KOH solution.

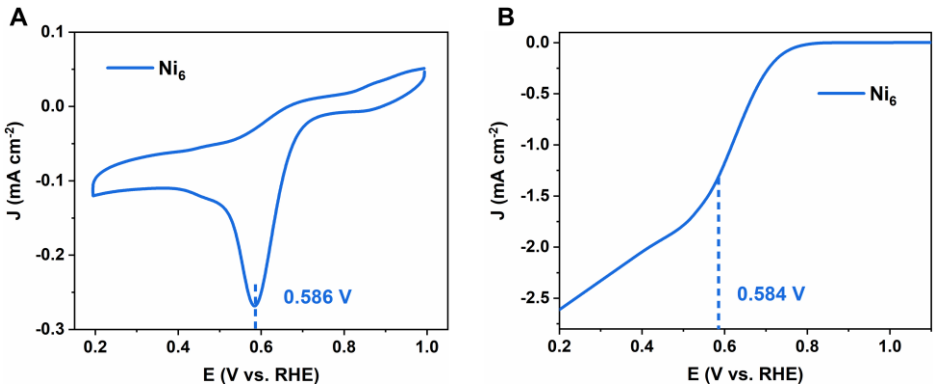

Figure S5. (A) CV curves of Ni_6 in O_2-saturated 0.1 M KOH. (B) LSV polarization curves of Ni_6 in 0.1 M KOH solution.

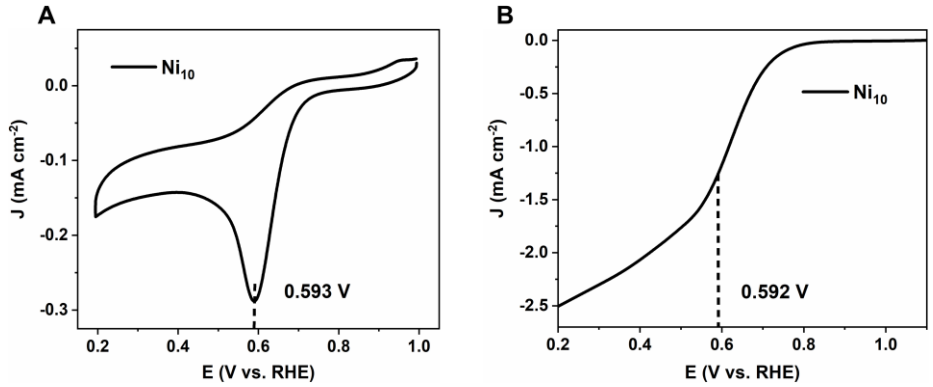

Figure S6. (A) CV curves of Ni_{10} in O_2-saturated 0.1 M KOH. (B) LSV polarization curves of Ni_{10} in 0.1 M KOH solution.

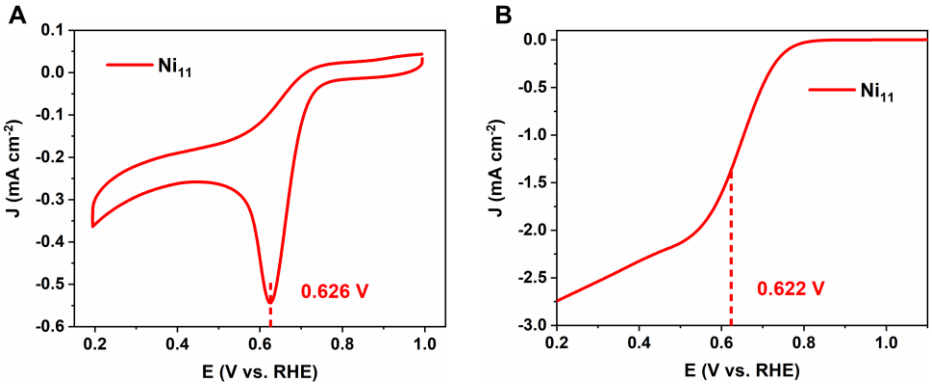

Figure S7. (A) CV curves of Ni_{11} in O_2-saturated 0.1 M KOH. (B) LSV polarization curves of Ni_{11} in 0.1 M KOH solution.

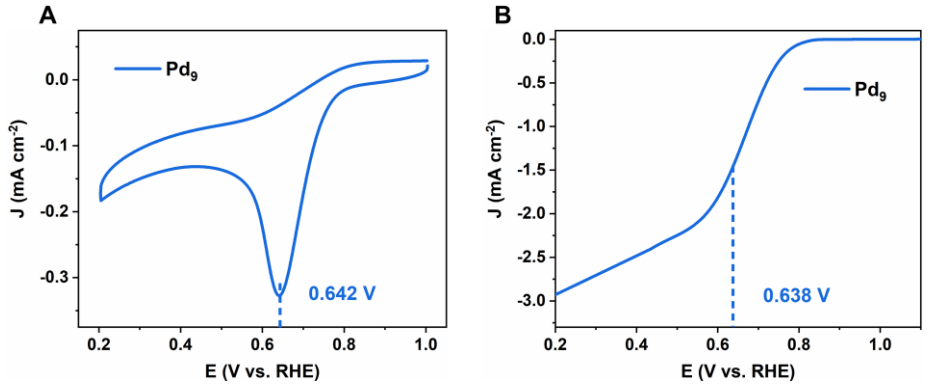

Figure S8. (A) CV curves of Pd_9 in O_2-saturated 0.1 M KOH. (B) LSV polarization curves of Pd_9 in 0.1 M KOH solution.

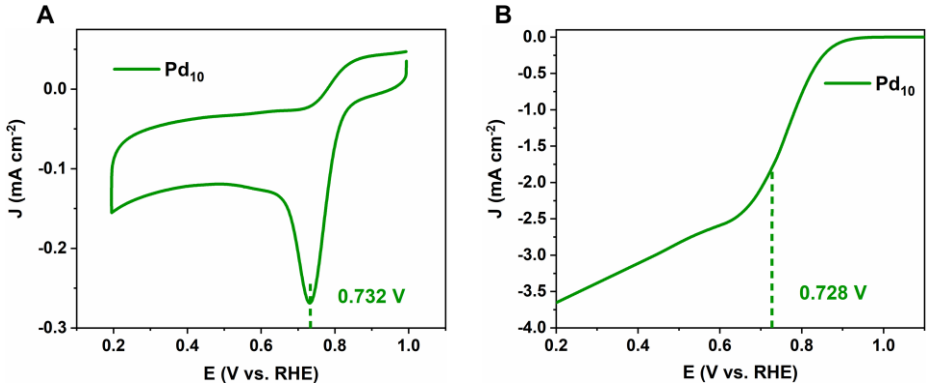

Figure S9. (A) CV curves of Pd_{10} in O_2-saturated 0.1 M KOH. (B) LSV polarization curves of Pd_{10} in 0.1 M KOH solution.

(4) Stability of $Ni_{11}(PhS)_{22}$, $Ni_{10}(4\text{-}MePhS)_{20}$, $Pd_9(SPh)_{18}$ and $Pd_{10}(SPh)_{20}$

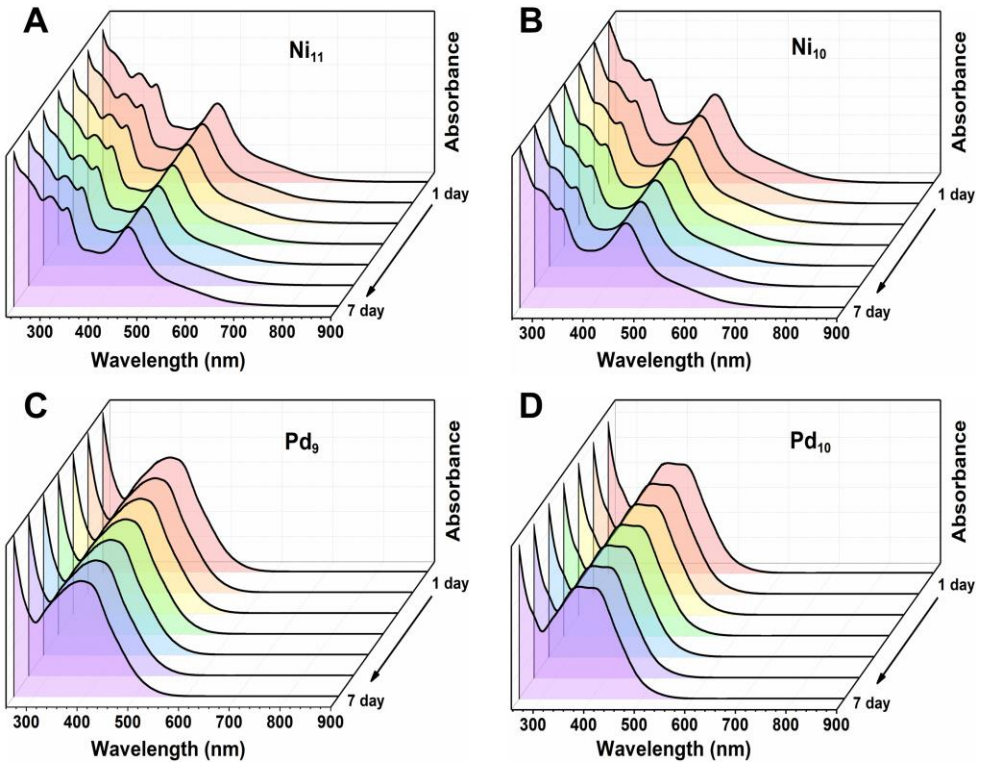

Figure S10. Time-dependent UV-vis spectra of Ni_{11} (A), Ni_{10} (B), Pd_9 (C), Pd_{10} (D).

(5) Stability of $Ni_{11}(PhS)_{22}$ under the alkaline condition

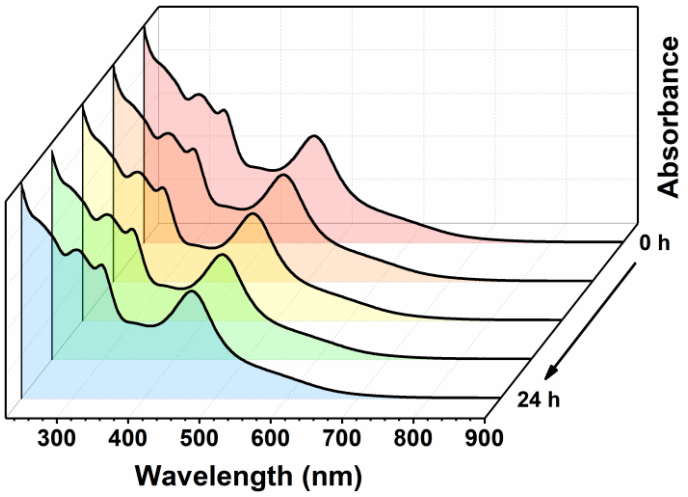

Figure S11. Time-dependent UV-vis spectra of Ni_{11} in aq. KOH (0.1 M).

(6) Structural and catalytic stability of $Pd_{10}(SPh)_{20}$ during catalysis

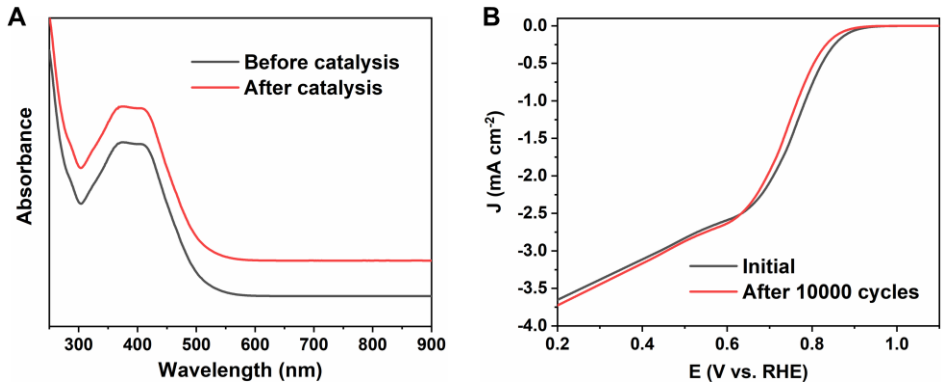

Figure S12. (A) Structural stability tests of Pd_{10}. (B) Catalytic stability tests of Pd_{10}.

(7) Structural and catalytic stability of $Ni_{10}(4\text{-}MePhS)_{20}$ during catalysis

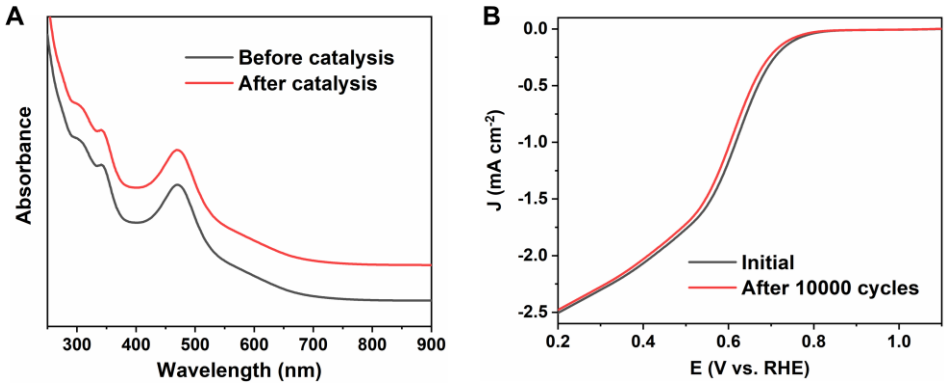

Figure S13. (A) Structural stability tests of Ni_{10}. (B) Catalytic stability tests of Ni_{10}.

(8) Structural and catalytic stability of $Pd_9(SPh)_{18}$ during catalysis

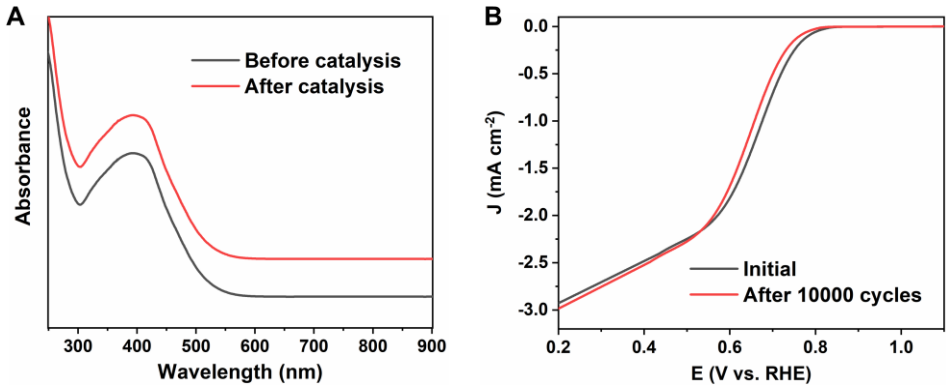

Figure S14. (A) Structural stability tests of Pd_9. (B) Catalytic stability tests of Pd_9.

Table S1. The corresponding distances and angles of Ni-Ni, S-S, Ni-S-Ni and S-Ni-S in $Ni_{11}(SPh)_{22}$ nanocluster.

Ni-Ni distances (Å)	S-S distances (Å)	Ni-S-Ni angles (°)	S-Ni-S angles (°)
2.955	2.93	84.61	82.95
2.955	2.92	83.63	83.14
3.193	2.917	93.02	82.65
2.834	2.881	93.65	83.35
2.858	2.951	80.18	84
3.215	2.951	79.87	78.61
2.856	2.881	81.07	78.61
3.215	2.917	80.47	84
2.858	2.920	94.24	83.35
2.834	2.930	93.95	82.65
3.193	2.787	80.94	83.14
avg: 2.99	avg: 2.91	80.94	82.95
		93.95	82.78
		94.24	82
		80.47	82.09
		81.07	84.11
		79.87	83.85
		80.18	83.85
		93.65	84.11
		93.02	82.95
		83.63	83.14
		84.61	82.65
		avg: 86.0	avg: 82.7

Crystal data

Table S2. Crystal data and structure refinement for $Ni_{11}(SPh)_{22}$

Empirical formula	$C_{132}H_{110}Ni_{11}S_{22}$
CCDC code	2292922
Formula weight	3047.28
Temperature/K	273.15
Crystal system	monoclinic
Space group	C2/c
a/Å	18.984(4)
b/Å	28.994(6)
c/Å	28.216(6)
α/°	90
β/°	99.45(3)
γ/°	90
Volume/Å^3	15320(6)
Z	4
ρ_{calc}g/cm^3	1.395
μ/mm^{-1}	5.190
F(000)	6584.0
Radiation	CuKα (λ = 1.54178)
2θ range for data collection/°	8.808 to 140.622
Index ranges	-21 ⩽ h ⩽ 23, -34 ⩽ k ⩽ 34, -32 ⩽ l ⩽ 12
Reflections collected	45301
Independent reflections	13994 [R_{int} = 0.0226, R_{sigma} = 0.0258]
Data/restraints/parameters	13994/1166/785
Goodness-of-fit on F^2	1.055
Final R indexes [I>=2σ (I)]	R_1 = 0.0681, wR_2 = 0.2096
Final R indexes [all data]	R_1 = 0.0761, wR_2 = 0.2183
Largest diff. peak/hole / e Å^{-3}	1.53/-1.25

Table S3. Crystal data and structure refinement for $Pd_{10}(SPh)_{20}$

Empirical formula	$C_{120}H_{100}Pd_{10}S_{20}$
CCDC code	2292923
Formula weight	3247.52
Temperature/K	296.15
Crystal system	triclinic
Space group	P-1
a/Å	15.8258(18)
b/Å	16.279(2)
c/Å	16.292(2)
α/°	64.679(4)
β/°	77.271(4)
γ/°	69.706(5)
Volume/Å^3	3545.6(8)
Z	1
ρ_{calc}g/cm^3	1.560
μ/mm^{-1}	1.609
F(000)	1640.0
Radiation	MoKα (λ = 0.71073)
2θ range for data collection/°	4.526 to 55.204
Index ranges	-20 ⩽ h ⩽ 20, -19 ⩽ k ⩽ 21, -21 ⩽ l ⩽ 21
Reflections collected	33637
Independent reflections	16254 [R_{int} = 0.0385, R_{sigma} = 0.0561]
Data/restraints/parameters	16254/1430/676
Goodness-of-fit on F^2	1.029
Final R indexes [I>=2σ (I)]	R_1 = 0.0434, wR_2 = 0.1021
Final R indexes [all data]	R_1 = 0.0600, wR_2 = 0.1110
Largest diff. peak/hole / e Å^{-3}	2.51/-1.39

Table S4. Crystal data and structure refinement for $Ni_{10}(4\text{-MePhS})_{20}$

Empirical formula	$C_{140}H_{140}Ni_{10}S_{20}$
CCDC code	2292924
Formula weight	3050.79
Temperature/K	273.15
Crystal system	orthorhombic
Space group	Fddd
a/Å	23.4478(13)
b/Å	30.2351(16)
c/Å	48.070(3)
α/°	90
β/°	90
γ/°	90
Volume/Å^3	34079(3)
Z	8
ρ_{calc}g/cm^3	1.205
μ/mm^{-1}	3.760
F(000)	12800.0
Radiation	CuKα (λ = 1.54178)
2θ range for data collection/°	7.294 to 139.85
Index ranges	-28 ⩽ h ⩽ 17, -34 ⩽ k ⩽ 36, -58 ⩽ l ⩽ 47
Reflections collected	60663
Independent reflections	7980 [R_{int} = 0.0778, R_{sigma} = 0.0394]
Data/restraints/parameters	7980/1044/412
Goodness-of-fit on F^2	1.026
Final R indexes [I>=2σ (I)]	R_1 = 0.0487, wR_2 = 0.1357
Final R indexes [all data]	R_1 = 0.0688, wR_2 = 0.1462
Largest diff. peak/hole / e Å^{-3}	0.45/-0.43

Table S5. Crystal data and structure refinement for $Pd_9(SPh)_{18}$

Empirical formula	$C_{108}H_{90}Pd_9S_{18}$
CCDC code	2292925
Formula weight	2922.77
Temperature/K	193.0
Crystal system	triclinic
Space group	P-1
a/Å	15.4893(15)
b/Å	17.1391(16)
c/Å	27.979(3)
α/°	73.147(4)
β/°	85.831(5)
γ/°	88.799(5)
Volume/Å^3	7089.8(12)
Z	2
ρ_{calc}g/cm^3	1.449
μ/mm^{-1}	1.491
F(000)	3048.0
Radiation	MoKα (λ = 0.71073)
2θ range for data collection/°	2.482 to 51.006
Index ranges	-18 ⩽ h ⩽ 18, -20 ⩽ k ⩽ 20, -33 ⩽ l ⩽ 33
Reflections collected	67310
Independent reflections	25851 [R_{int} = 0.0819, R_{sigma} = 0.0983]
Data/restraints/parameters	25851/0/1223
Goodness-of-fit on F^2	1.062
Final R indexes [I>=2σ (I)]	R_1 = 0.0987, wR_2 = 0.2794
Final R indexes [all data]	R_1 = 0.1555, wR_2 = 0.3172
Largest diff. peak/hole / e Å^{-3}	2.20/-1.80

References

[1] M. Zhu, S. Zhou, C. Yao, L. Liao, Z. Wu, *Nanoscale.* **2014**, 6, 14195-14199.